Environmental Science & Technology

Article

Cite This: Environ. Sci. Technol. 2017, 51, 13170-13179

pubs.acs.org/est

Carbon, Hydrogen, and Nitrogen Isotope Fractionation Trends in *N*-Nitrosodimethylamine Reflect the Formation Pathway during Chloramination of Tertiary Amines

Stephanie Spahr,[†,‡,∥] Urs von Gunten,[†,‡,§] and Thomas B. Hofstetter*[,†,§]

[†]Eawag, Swiss Federal Institute of Aquatic Science and Technology, CH-8600 Dübendorf, Switzerland

[‡]School of Architecture, Civil and Environmental Engineering (ENAC), Ecole Polytechnique Federale de Lausanne (EPFL), CH-1015 Lausanne, Switzerland

[§]Institute of Biogeochemistry and Pollutant Dynamics, ETH Zürich, CH-8092 Zürich, Switzerland

Supporting Information

ABSTRACT: Assessing the precursors and reactions leading to the carcinogenic *N*-nitrosodimethylamine (NDMA) during drinking water disinfection is a major challenge. Here, we investigate whether changes of $^{13}C/^{12}C$, $^{2}H/^{1}H$, and $^{15}N/^{14}N$ ratios of NDMA give rise to isotope fractionation trends that can be used to infer NDMA formation pathways. We carried out compound-specific isotope analysis (CSIA) of NDMA during chloramination of four tertiary amines that produce NDMA at high yields, namely ranitidine, 5-(dimethylaminomethyl)furfuryl alcohol, *N*,*N*-dimethylthiophene-2-methylamine, and *N*,*N*-dimethylbenzylamine. Carbon and hydrogen isotope ratios of NDMA function as fingerprints of the $N(CH_3)_2$ moiety and exhibit only minor isotope fractionation during the disinfection process. Nitrogen isotope ratios showed that NH_2Cl is the source of the N atom of the nitroso group. The large enrichment of ^{15}N in NDMA was indicative of the isotope effects pertinent to bond-cleavage and bond-formation reactions during chloramination of the tertiary amines. Correlation of $\delta^{15}N$ versus $\delta^{13}C$ values of NDMA resulted in trend lines that were not affected by the type of tertiary amine and treatment conditions, suggesting that the observed C and N isotope fractionation in NDMA may be diagnostic for NDMA precursors and formation pathways during chloramination.

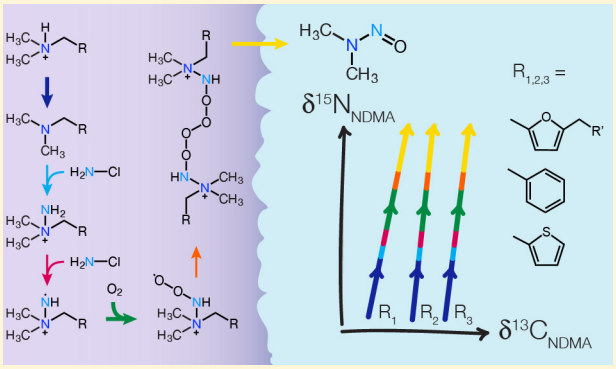

INTRODUCTION

N-Nitrosamines form as drinking water disinfection byproducts (DBPs) and are of public and regulatory concern due to their mutagenicity and potential carcinogenicity.[1,2] *N*-Nitrosodimethylamine (NDMA) is a frequently detected DBP in finished drinking waters and often exceeds guidance values of 9−100 ng/L.[2−5] NDMA is produced unintentionally with typically used disinfectants, that is, chlorine, chloramine, and ozone, through reactions with organic compounds in raw waters including natural organic matter,[6−9] anthropogenic contaminants such as pharmaceuticals and pesticides,[10−14] and chemicals used for water treatment (e.g., polymeric coagulants).[15,16] The different molecular structures of NDMA precursors have led to the conclusion that pathways of NDMA generation differ widely among the various disinfection procedures.[17,18] Nevertheless, detailed knowledge of chemical reaction mechanisms remains scarce so that a systematic prediction and prevention of NDMA formation during water treatment is currently hampered.

One promising new tool with which NDMA can be related to its precursors and formation reactions is compound-specific isotope analysis (CSIA). Previous studies have demonstrated that changes in the natural stable isotope composition of DBPs, that is the so-called stable isotope fractionation, provide evidence for reactive precursor materials and DBP formation pathways.[19−21] CSIA was applied, for example, to monitor changes of $^{13}C/^{12}C$ ratios in chloroform produced upon chlorination of lake water.[19] Chloroform was enriched in ^{12}C due to a preferential reaction of light (i.e., ^{12}C-containing) isotopologues when produced from resorcinol-like moieties of natural organic matter (NOM). Conversely, chloroform was enriched in ^{13}C when generated from chlorination of phenolic functional groups of NOM. These contrasting isotopic preferences reflect different chloroform formation pathways. Each of these exhibits different kinetic isotope effects (KIEs), which reflect which chemical bonds are broken and formed.[22,23] Because KIEs are specific features of a reaction mechanism, the stable isotope fractionation

Received: August 1, 2017
Revised: October 5, 2017
Accepted: October 15, 2017
Published: October 16, 2017

DOI: 10.1021/acs.est.7b03919
Environ. Sci. Technol. 2017, 51, 13170−13179

observed in the reactants and products can serve as proxy for the transformation pathway.[24−28]

We have recently introduced analytical procedures for $^{13}C/^{12}C$, $^{2}H/^{1}H$, and $^{15}N/^{14}N$ isotope ratio measurements of *N*-nitrosamines.[29] However, this method has not been applied to study disinfection processes and it is currently unknown how C, H, and N isotope fractionation in NDMA can be indicative of its formation pathway(s). Elucidation of reaction mechanisms with CSIA typically focuses on the analysis of substrate disappearance, in which substrate isotope fractionation reveals the isotope effects of the first elementary reaction steps leading to irreversible bond cleavage(s).[24−27] Gaining such information from product isotope fractionation is less common and CSIA of reaction products is applied mostly to study the isotope effects of well-defined reactions leading to known and measurable products (e.g., refs 30−34). None of the previous applications of CSIA reflect cases similar to the one of NDMA, which forms in a sequence of (partially) unknown reactions. Each of these reactions exhibits an isotope effect and thus contributes to the final isotopic composition of NDMA.[11,35] However, the identification of reactive processes from the isotope fractionation in reaction products is a common approach in (bio)geosciences. In this discipline, the elucidation of events in the past is often made through isotopic analysis of frequently occurring molecules and minerals in natural samples such as hydrocarbons, sulfur species, oxides, and carbonates.[36,37] The methodology is based on observations made in multiple isotope systems, that is from the comparison of isotope fractionation from different elements in a molecule (e.g., $^{2}H/^{1}H$ versus $^{13}C/^{12}C$ in methane and $^{18}O/^{16}O$ versus $^{34}S/^{32}S$ in sulfate) and different isotopes of the same elements (e.g., $^{18}O/^{16}O$ versus $^{17}O/^{16}O$ in O_2 and $^{34}S/^{32}S$ versus $^{33}S/^{32}S$ in sulfates).[38−43] Regardless of a quantitative understanding of isotope effects of individual reactions, evidence for reactive processes can then be obtained from correlations of isotope fractionation, which, in most cases, result in indicative isotope fractionation trendlines.

The objective of this work was to evaluate whether multielement isotope fractionation analysis is applicable to track precursor moieties and formation pathways of NDMA through analysis of C, H, or N isotope ratios of the DBP. This work builds on two of our recent studies on the NDMA formation from the chloramination of tertiary amines[29,35] and information on the reaction mechanism provided by others.[17,44−46] Based on the evidence of radical intermediates and reactions of molecular oxygen in the NDMA formation pathway,[35] we hypothesized that tertiary amines undergo a sequence of substitution, electron transfer, oxygenation, and radical coupling reactions shown in Scheme 1. Those reactions will be the source of isotope fractionation in NDMA. In our previous work on stable isotope analysis,[29] we have used the chloramination reaction of ranitidine to validate our methodology, and we found that NDMA formation processes can be studied at low μM concentrations if NDMA yields are high. Therefore, we focused our current investigation on chloramination of tertiary amines, which can give rise to yields of NDMA that exceed 60%.[11,14,29,35,47] We conducted chloramination experiments with four tertiary amines, namely ranitidine, 5-(dimethylaminomethyl)-furfuryl alcohol (DFUR), *N,N*-dimethylthiophene-2-methylamine (DMTA), and *N,N*-dimethylbenzylamine (DMBA; see Scheme 1), and investigated C, H, and N isotope fractionation in NDMA during its formation from these precursors. First, we inferred the sources of C, H, and N atoms in NDMA by examining the initial and site-specific isotope ratios of

Scheme 1. NDMA Formation Pathway during the Chloramination of Selected Tertiary Amines (Adapted from Spahr et al.[35]), Including the Precursor Compounds Examined in This Study (Ranitidine, DFUR, DMTA, and DMBA)[a]

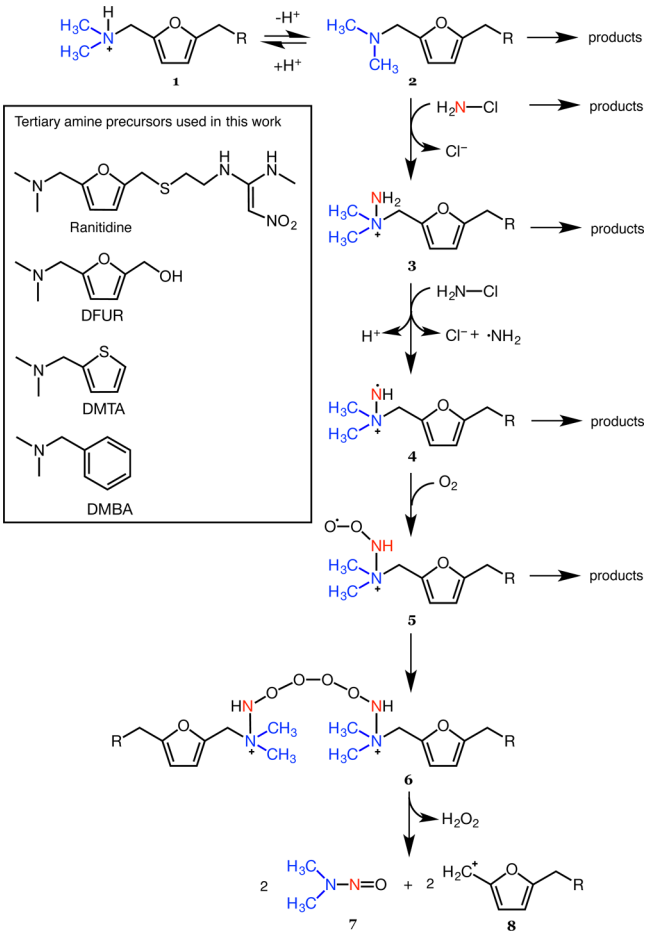

[a]At pH 8.0 deprotonation of tertiary amines (**1** to **2**) occurs prior to nucleophilic attack on NH_2Cl. Reactive intermediates include substituted dimethylhydrazines (**3**), aminyl radicals (**4**), *N*-peroxyl radicals (**5**), and tetroxide species (**6**). Decomposition of **6** leads to two equivalents of NDMA (**7**) and carbocations (**8**). Based on a molar NDMA yield of <100%, precursors or intermediates **3**−**5** also undergo reactions to unidentified products.

selected precursors and by conducting experiments with isotopically distinct monochloramines. Second, we investigated to which extent the C and N isotope fractionation trends in two model tertiary amines and NDMA reflect NDMA formation pathways involving multiple isotope-sensitive reaction steps. Finally, we assessed whether the multielement isotope fractionation trends of NDMA are characteristic for chloramination of tertiary amines and could potentially be used as a proxy for the NDMA formation pathway during drinking water disinfection.

EXPERIMENTAL SECTION

Chemicals. A list of all chemicals including suppliers and purities is provided in the Supporting Information (SI).

NDMA Formation Experiments. Monochloramine (NH_2Cl) stock solutions (30 mM) were prepared daily as described previously[48,49] by mixing hypochlorite (OCl^-) with either ammonium chloride (NH_4Cl) or ammonium sulfate ($(NH_4)_2SO_4$) at pH 9.5 with a molar Cl:N ratio of 1:1.05. The ammonium

DOI: 10.1021/acs.est.7b03919
Environ. Sci. Technol. 2017, 51, 13170−13179

salts exhibited distinctly different and well-defined N isotope ratios corresponding to N isotope signatures, $\delta^{15}N$, of −1.4‰ and +53.7‰ for NH_4Cl and $(NH_4)_2SO_4$, respectively.[50]

Chloramination experiments were carried out in 14 amber glass bottles containing 1 L of either 10 mM phosphate buffer (pH 8.0), 10 mM phosphate buffer (pH 7.0), 50 mM phosphate buffer (pH 8.0), or 10 mM borate buffer (pH 8.0). Each reactor was spiked with 100 μL of a methanolic stock solution to obtain initial concentrations of 3 μM ranitidine or DFUR and 40 μM DMTA or DMBA. The formation of NDMA was initiated through the addition of NH_2Cl in 15-fold excess corresponding to initial NH_2Cl concentrations of 45 or 600 μM, respectively. At predefined time points, one 1 L reactor was sacrificed for chemical analyses. We measured the solution pH and NH_2Cl concentration, and quenched the chloramine reaction by adding 0.5 g of $Na_2S_2O_3$ to the reactor. To quantify the concentrations of NDMA, ranitidine, and DFUR, 1 mL of the solution was filled into an 1.5 mL amber autosampler glass vial. For analyses of DMTA and DMBA, 40 mL of the solution was transferred into 50 mL amber glass flasks, and the pH of the solution was adjusted to 11.3 through addition of 5 M NaOH. All samples were stored in the dark at 4 °C until concentration analyses and further processing for stable isotope analyses. Two control experiments were set up (i) to quantify losses of the organic amine precursor in the absence of NH_2Cl and (ii) to determine the self-decay rate of NH_2Cl in the absence of organic amines. Unless stated otherwise, reported NH_2Cl concentrations were corrected by the self-decay of NH_2Cl. The presence of methanol had no effect on the consumption of NH_2Cl and the formation of NDMA as shown previously.[35]

Chemical Analyses. The concentration of aqueous NH_2Cl stock solutions (30 mM) was quantified as described previously using a Varian Cary 100 Bio UV-visible spectrophotometer.[29,48,49,51] In reaction mixtures containing tertiary amines, reactive intermediates, and NDMA, NH_2Cl was quantified with a colorimetric method using 2,2′-azino-bis(3-ethylbenzothiazoline-6-sulfonic acid) diammonium salt (ABTS).[29,52] A detailed comparison of chloramine quantification methods can be found in section S5 in the Supporting Information for Spahr et al.[35] Concentrations of NDMA, ranitidine, and DFUR were determined by reverse-phase HPLC with UV detection (Dionex UltiMate 3000).[29,35]

Concentrations of DMTA and DMBA were measured by solid-phase microextraction (SPME) coupled to a gas chromatograph-mass spectrometer (GC/MS) (Thermo TRACE GC Ultra and Thermo TRACE DSQ II). Amber autosampler glass vials (2 mL), which contained 0.3 g NaCl, were filled with 1.3 mL of aqueous sample in 10 mM phosphate buffer (pH 11.3) and shaken on a Vortex mixer. Direct immersion SPME was carried out with a polydimethylsiloxane/divinylbenzene-coated fiber (PDMS/DVB, 65 μm, Supelco) after the fiber was conditioned daily for 30 min at 250 °C. Analytes were extracted for 45 min at 40 °C and desorbed within 3 min at 270 °C in the split/splitless injector of the GC.[53] The GC was equipped with 1 m DPTMDS (methyl/phenyl) deactivated fused-silica guard column (0.53 mm i.d., BGB) and a 30 m × 0.25 mm ZB-5ms column (0.25 μm, Zebron, Phenomenex). Helium carrier gas was used at a constant pressure of 130 kPa. The temperature program was 1 min at 50 °C, 10 °C/min to 250 °C, and 5 min at 250 °C. DMTA and DMBA concentrations were quantified with an external calibration of 0.1−1.5 μM.

Stable Isotope Analyses. Stable C, H, and N isotope ratios of NDMA were measured using gas chromatography-isotope ratio mass spectrometry (GC/IRMS) coupled to solid-phase extraction (SPE), as reported in Spahr et al.[29] C and N isotope analysis of DMTA and DMBA in aqueous samples was conducted with SPME-GC/IRMS. The SPME procedure, GC setup, and temperature program was identical to that for GC/MS analysis, but a 30 m × 0.32 mm ZB-5ms column (1 μm, Zebron, Phenomenex) was used. For all C and N isotope measurements, a Ni/Ni/Pt reactor was operated at 1000 °C.[29] Method quantification limits (MQLs) of the SPME-GC/IRMS measurements of DMTA and DMBA were determined according to the moving mean procedure of Jochmann et al.,[54] and measurements were made in concentration ranges of 0.3−0.6 and 2.5−16 μM for DMTA and DMBA, respectively (Figure S1). The ^{15}N equilibrium isotope effect associated with the deprotonation of DMTA was investigated by SPME-GC/IRMS at pH 8.4, 8.7, 9.4, 10.4, and 11.3 in 10 mM phosphate buffer at ionic strength of 4 M using DMTA concentrations of 66, 12 (pH 8.7 and 9.4), 6.6, and 5 μM, respectively.[53]

Carbon, hydrogen, and nitrogen isotope ratios are reported as $\delta^{13}C$, $\delta^{2}H$, and $\delta^{15}N$ relative to Vienna PeeDee Belemnite, Vienna standard mean ocean water, and air, respectively.[24,29] All isotope signatures are reported in permil (‰) as arithmetic mean of triplicate measurements ($\pm\sigma$). To ensure the accuracy of the measured isotope ratios, we used a series of isotopic standard materials purchased from Indiana University,[55,56] as documented in Spahr et al.,[29] as well as calibrated in-house standards in standard bracketing procedures. In-house standards of ranitidine, DFUR, DMTA, and NH_4Cl were obtained through C and N isotope ratio measurements with an elemental analyzer IRMS (Table S1). Isotopic analysis of NH_2Cl was impeded owing to its thermal instability and self-decay to ammonia. Instead, we used the $\delta^{15}N$ values of NH_4Cl or $(NH_4)_2SO_4$, from which NH_2Cl was produced, as a proxy for the initial $\delta^{15}N$ values of NH_2Cl. This assumption was based on high molar NH_2Cl yields (>94%) from the reaction of HOCl with NH_4Cl or $(NH_4)_2SO_4$.

Data Evaluation. We conducted chloramination experiments with two model compounds, namely DMTA and DMBA, to study isotope fractionation in the tertiary amines. Bulk isotope enrichment factors for carbon and nitrogen, ε_C and ε_N, were derived from linear regression of $\delta^{13}C$ and $\delta^{15}N$ values versus fractional amount of remaining precursor (c/c_0) according to eq 1 (see Figure S3):[25]

$$\ln\left(\frac{\delta^{h}E + 1}{\delta^{h}E_0 + 1}\right) = \varepsilon_E \cdot \ln\left(\frac{c}{c_0}\right) \quad (1)$$

where $\delta^{h}E_0$ and $\delta^{h}E$ are isotope ratios of an element E in the precursor at the beginning and during the reaction, respectively. Apparent kinetic isotope effects, $AKIE_E$, were calculated according to eq 2 considering the total number of atoms of an element (n), the number of atoms in reactive positions (x), and the number of atoms in intramolecular competition (z). The $AKIE_C$ values are reported as average secondary isotope effect for all C atoms in DMTA ($n = x = 7$, $z = 1$) and DMBA ($n = x = 9$, $z = 1$). $AKIE_N$ values stand for primary isotope effects and both precursors contain one N atom ($n = x = z = 1$). Uncertainties of ε_E and $AKIE_E$ values are reported as a 95% confidence interval:

$$AKIE_E = \frac{1}{1 + (n/x)\cdot z\cdot \varepsilon_E} \quad (2)$$

DOI: 10.1021/acs.est.7b03919
Environ. Sci. Technol. 2017, 51, 13170−13179

The observable $AKIE_N$ of DMTA or DMBA during chloramination at pH 8.0 originates from the combination of a deprotonation step (eq 3) and the subsequent reaction of the neutral tertiary amine (eq 4). As we have shown previously,[53,57] the observable $AKIE_N$ therefore consists of a combination of a ^{15}N-equilibrium isotope effect for the quarternary amine deprotonation, $EIE_N^{BH^+-B}$ and an apparent kinetic isotope effect of the subsequent reaction, $AKIE_N^B$ (eq 5):

$$BH^+ \underset{k_{-1}}{\overset{k_1}{\rightleftharpoons}} B + H^+ \quad (3)$$

$$B \xrightarrow{k_2} P \quad (4)$$

$$AKIE_N = f_{BH^+} \cdot EIE_N^{BH^+-B} \cdot AKIE_N^B + (1 - f_{BH^+}) \cdot AKIE_N^B \quad (5)$$

where k_1 and k_{-1} are rate constants of H^+ exchange reaction, k_2 is the rate constant for transformation of the neutral amine, and f_{BH^+} is the fraction of the conjugate acid of the tertiary amine (see section S4 in the Supporting Information for details).

RESULTS AND DISCUSSION

Observable C, H, and N Isotope Fractionation Trends in NDMA. We used 5-(dimethylaminomethyl)furfuryl alcohol (DFUR) as model compound for the chloramination of tertiary amines and studied the NDMA formation kinetics as well as the C, H, and N isotope ratios of NDMA. Figure 1a shows the formation of NDMA during the reaction of DFUR (3 μM) with NH_2Cl (45 μM) in 10 mM phosphate buffer at pH 8.0. The reaction was completed within 10 h with a molar NDMA yield of 65 ± 2%.[35,47,58] Consistent with our earlier observations, we found a lag phase of approximately 1 h, in which only 0.2 μM DFUR was transformed to 0.1 μM NDMA (dashed line in Figure 1a).[35] After 1 h, DFUR disappeared at a faster rate concomitant with the formation of NDMA. This kinetic behavior implies that reactive intermediates such as the *N,N*-dimethylhydrazine species (compound **3** in Scheme 1) and possible radical intermediates (**4** and **5**) are short-lived and transformed to NDMA and other unidentified products more rapidly than the initial transformation of DFUR to compound **3**. The total consumption of NH_2Cl amounted to 12.0 μM and thus exceeded the initial concentration of DFUR by a factor of 4.1, in agreement with previous findings.[35] No lag phase was observed for the disappearance of NH_2Cl (Figure 1a), indicating that side reactions, which did not lead to NDMA, likely contributed to the overstoichiometric consumption of NH_2Cl.

Figure 1b shows C, H, and N isotope signatures of NDMA during its formation. The $\delta^{15}N$ values of NDMA (depicted as upward triangles) increased within 10 h from −24.8‰ to −8.7‰. This N isotope fractionation is caused by primary kinetic isotope effects that occur when chemical bonds to N are broken or formed in rate-determining reaction steps.[25,59] In contrast, $\delta^{13}C$ and δ^2H values of NDMA changed only slightly from −36.8‰ to −34.3‰ and from −133.5‰ to −110.7‰, respectively. This C and H isotope fractionation is small compared to reactions, in which bonds to C and H are broken (e.g, refs 60 and 61) and is likely due to secondary kinetic isotope effects of atoms that do not participate in chemical reactions.

Isotope Ratios of NDMA Reveal the Origin of C, H, and N Atoms in NDMA. *Origin and Isotopic Composition of the N,N-Dimethylamine Moiety of NDMA.* We have shown previously that the *N,N*-dimethylamine group ($N(CH_3)_2$) of the tertiary amine is transferred to NDMA without being chemically altered.[29] This observation was key to elucidate the mechanisms of N atom oxygenation and formation of radical intermediates in the NDMA formation pathway[35] and is also of critical importance to assess the C, H, and N isotope fractionation associated in NDMA in the present study (see below).

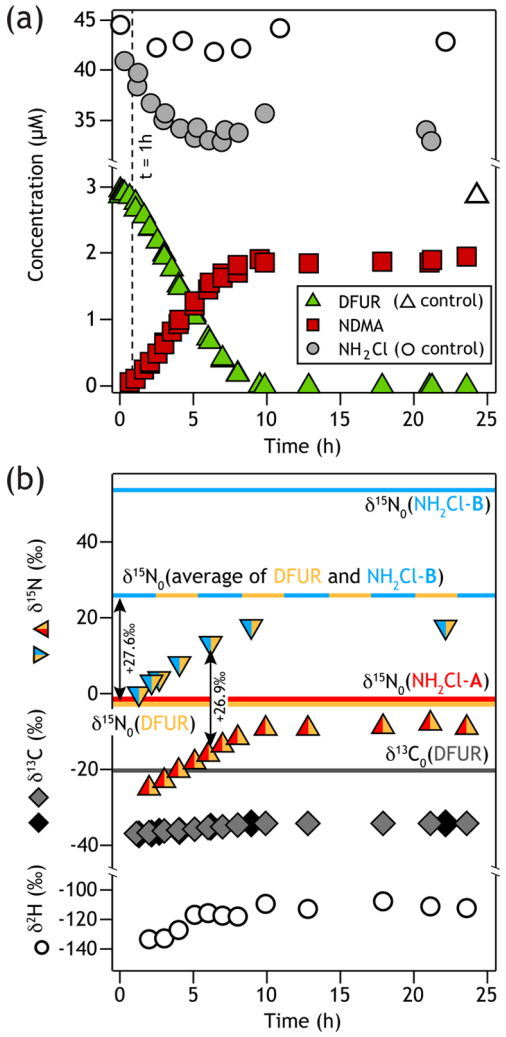

Figure 1. NDMA formation from the reaction of DFUR (3 μM) with NH_2Cl (45 μM) in 10 mM phosphate buffer (pH 8.0). Panel (a) shows DFUR abatement, NH_2Cl consumption, and NDMA formation over time. The symbols in panel (b) illustrate $\delta^{15}N$, $\delta^{13}C$, and δ^2H values of NDMA. Gray and yellow solid lines represent the initial $\delta^{13}C$ and $\delta^{15}N$ value of DFUR, respectively. The red and blue lines depict the initial $\delta^{15}N$ values of two different NH_2Cl batches with which separate NDMA formation experiments were conducted leading to NDMA with different $\delta^{15}N$ signatures (red−yellow vs blue−yellow triangles). The blue−yellow line represents the average of the initial $\delta^{15}N$ values of DFUR and NH_2Cl-**B**. Standard deviations of triplicate $\delta^{15}N$, $\delta^{13}C$, and δ^2H measurements were <0.2‰, <0.4‰, and <5.0‰, respectively, and smaller than the depicted symbols.

The identical δ^2H values of the $N(CH_3)_2$ moiety in ranitidine and the δ^2H of NDMA reported earlier confirmed the accuracy of isotope ratio measurements by GC/IRMS.[29] This finding implied that the $\delta^{13}C$ value of NDMA also corresponds to the $\delta^{13}C$ value of the $N(CH_3)_2$ group of the tertiary amine. Similar to previous results for ranitidine, we observe here for DFUR that the final $\delta^{13}C$ value of NDMA (−34.3‰) was 14.5‰ more negative than the average $\delta^{13}C$ value of the 8 C atoms in the precursor molecule (−19.8‰, gray line in Figure 1b). The average $\delta^{13}C$ value of the C atoms in the furfuryl moiety

DOI: 10.1021/acs.est.7b03919
Environ. Sci. Technol. 2017, 51, 13170−13179

and methylene C was −14.9‰. This result confirms not only the uneven distribution of ^{12}C and ^{13}C atoms in the tertiary amine but also that ^{12}C atoms are preferentially found in the $N(CH_3)_2$ group.

Source of N Atoms in NDMA. N isotope signatures of NDMA reflect the average isotope ratios of both N atoms of NDMA and can reveal the sources of nitrogen. For the reasons outlined above, the N atom of the $N(CH_3)_2$ group stems from the tertiary amine, whereas the N atom of the nitroso group derives from NH_2Cl. However, simple N isotope mass balances would fail to show the origin of the N atoms because only 65% of DFUR was transformed to NDMA so that 35% of the N atoms ended up in unidentified products. Moreover, less than 5% of the N atoms of NH_2Cl were incorporated into NDMA (final concentration of 1.9 μM) because NH_2Cl was present in excess (initial concentration of 45 μM). The final $\delta^{15}N$ value of NDMA ($\delta^{15}N$ = −8.7‰) therefore does not match the average value of the initial N isotope signatures of DFUR ($\delta^{15}N_{DFUR}$ = −2.2‰, yellow line in Figure 1b) and monochloramine ($\delta^{15}N_{NH_2Cl-A}$ = −1.4‰, red line). Owing to the incomplete conversion of both precursors to NDMA and a preferential reaction of ^{14}N to NDMA caused by a normal N kinetic isotope effect, the final $\delta^{15}N$ value of NDMA (upward triangles in Figure 1b) was 6.9‰ more negative than the average N isotope signature of both precursors (−1.8‰).

To quantify the origin of N atoms in NDMA, we conducted a second, independent NDMA formation experiment with the same DFUR of known isotopic composition but with an isotopically distinctly different batch of monochloramine (NH_2Cl-**B**). NH_2Cl from batch **B** exhibited a $\delta^{15}N_{NH_2Cl-B}$ of +53.7‰ (blue line in Figure 1b) and was thus enriched in ^{15}N by +55.1‰ compared to NH_2Cl-**A** ($\delta^{15}N_{NH_2Cl-A}$ = −1.4‰). We observed the same extent of N isotope fractionation in NDMA regardless of whether NH_2Cl-**A** or NH_2Cl-**B** reacted with DFUR. $\delta^{15}N$ values of NDMA changed by +16.1‰ and +17.6‰, respectively, during its formation. Because of a $\delta^{15}N_{NH_2Cl-B}$ value of +53.7‰, $\delta^{15}N$ values of NDMA were shifted toward much more positive values (downward triangles in Figure 1b) compared to NDMA formed from NH_2Cl-**A**. The shift of $\delta^{15}N$ of NDMA due to the use of NH_2Cl-**B** instead of NH_2Cl-**A** amounted to +26.9 ± 2.2‰ (indicated as black arrows in Figure 1b). This offset corresponds to 50% (i.e., 27.6‰) of the difference of $\delta^{15}N$ between the two NH_2Cl batches (−1.4‰ vs −53.7‰) and, therefore, confirms that one N atom in NDMA originates from NH_2Cl and one N atom stems from the tertiary amine.[62] Note that $\delta^{13}C$ values of NDMA produced with NH_2Cl-**A** and NH_2Cl-**B** (gray and black diamonds, respectively, in Figure 1b) were identical, which is in agreement with the fact that both C atoms of the $N(CH_3)_2$ group of NDMA originate from DFUR.

Isotope Fractionation Trends of Tertiary Amines and NDMA Reflect the Multistep NDMA Formation Pathway. As illustrated in Scheme 1, NDMA formation is a multistep process, in which reactions of N atoms play a key role. Deprotonation of tertiary amines (compound **1** in Scheme 1) occurs prior to the initial reaction of **2** with NH_2Cl leading to a hydrazine-type intermediate (**3**).[44] Subsequently, the NH_2-group of **3** is oxidized to a N-centered radical **4** that reacts with aqueous O_2.[35] The final release of NDMA from compound **6** requires the formation of a nitroso moiety as well as the cleavage of a C−N bond to the methylene group of the tertiary amine. Because molar NDMA yields were smaller than 100%, tertiary amines or intermediate species also react to products other than NDMA. Every elementary reaction step depicted in Scheme 1 is associated with an isotope effect and can thus cause isotope fractionation in the precursors (tertiary amine and NH_2Cl) as well as in NDMA. In the following sections, we evaluate how these reactions contribute to the observable isotope fractionation in the tertiary amine and in NDMA.

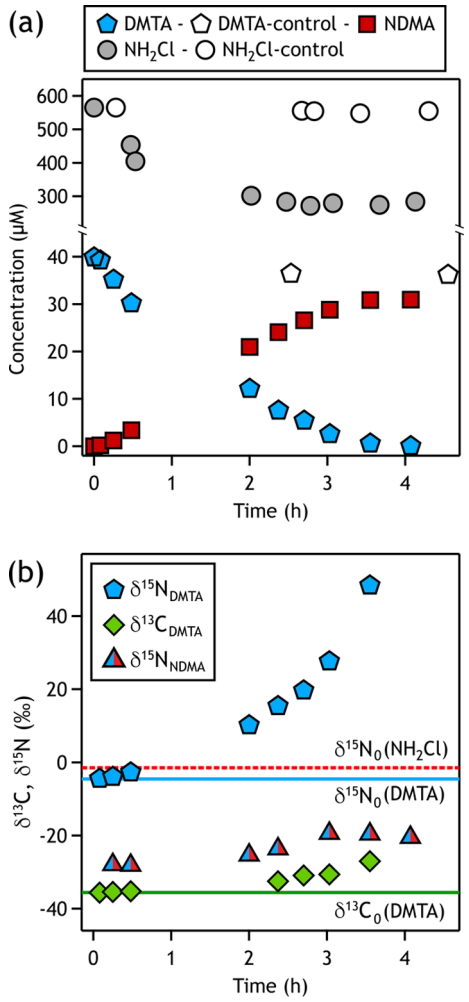

Figure 2. NDMA formation from the reaction of DMTA (40 μM) with NH_2Cl (600 μM) in 10 mM phosphate buffer at pH 8.0. Panel (a) shows DMTA degradation, NH_2Cl consumption, and NDMA formation over time. The symbols in panel (b) demonstrate $\delta^{13}C$ and $\delta^{15}N$ values of DMTA as well as $\delta^{15}N$ values of the formed NDMA during chloramination. Solid lines represent the initial $\delta^{13}C$ and $\delta^{15}N$ values of DMTA and NH_2Cl. Standard deviations of triplicate $\delta^{13}C$ and $\delta^{15}N$ measurements of DMTA and NDMA were <0.2‰ and <0.8‰, respectively, and smaller than the depicted symbols.

C and N Isotope Fractionation in Tertiary Amines. We studied C and N isotope fractionation in two tertiary amine model compounds, namely *N,N*-dimethylthiophene-2-methylamine (DMTA) and *N,N*-dimethylbenzylamine (DMBA) during chloramination. DMTA and DMBA are structurally similar to DFUR (Scheme 1), known to produce high NDMA yields,[47] and are, in contrast to DFUR, amenable to isotope analysis by GC/IRMS. Figure 2a shows the NDMA formation during the reaction of DMTA (40 μM) with NH_2Cl (600 μM) in 10 mM phosphate buffer at pH 8.0. Similar to the experiment with DFUR, NDMA formation was concurrent with the transformation of DMTA and consumption of NH_2Cl. After 4 h, 288 ± 6 μM NH_2Cl were consumed and NDMA was formed with a molar yield of 75.4 ± 0.1% in agreement with published data.[47] Chloramination of DMTA was accompanied by C and N isotope

DOI: 10.1021/acs.est.7b03919
Environ. Sci. Technol. 2017, 51, 13170−13179

fractionation in the remaining tertiary amine (Figure 2b). The $\delta^{13}C$ and $\delta^{15}N$ values of DMTA changed by +8.6‰ and +52.9‰, respectively, demonstrating that precursor molecules containing ^{12}C and ^{14}N reacted preferentially. This isotopic preference corresponds to apparent ^{13}C and ^{15}N kinetic isotope effects of 1.0021 ± 0.0003 ($AKIE_C$) and 1.0127 ± 0.0007 ($AKIE_N$) derived from eqs 2 and 5 (see details in section S4 and Table S2).

The notable extent of N isotope fractionation in DMTA reflects the N isotope effects of all reactions of the reactant and its transient products up to and including the first irreversible step in the reaction sequence. However, only few isotope effects of the reactions shown in Scheme 1 have been studied in independent experiments and the rate-limiting steps of the chloramination of tertiary amines to NDMA are not known. The reaction kinetics shown in Figures 1a and 2a suggest that the disappearance of the tertiary amine and formation of NDMA occur simultaneously without the formation of long-lived intermediates. Therefore, we hypothesize that one rate-determining step governs the kinetics of tertiary amine disappearance and formation of NDMA. This step could be the formation of the hydrazine intermediate (**2** → **3**) or the formation of the N-centered radical (**3** → **4**). Reactions **4** → **5** and **5** → **6** involve radical species and are likely irreversible and faster than the preceding reaction steps. Given that approximately 98% of the DMTA molecules are protonated at pH 8.0, the H^+ exchange reaction **1** ⇌ **2** may also contribute to the observable N isotope fractionation in DMTA. It is thus likely that reactions **1** ⇌ **2** → **3** or **1** ⇌ **2** ⇌ **3** → **4** are the source of N isotope fractionation in the reactant. Indeed, the deprotonation of conjugate acids of *N,N*-dimethylaniline and substituted anilines gives rise to a ^{15}N equilibrium isotope effect, $EIE_N^{BH^+-B}$, of 1.014 to 1.0203.[53,63,64] For the deprotonation of DMTA, we determined an $EIE_N^{BH^+-B}$ of 1.0103 ± 0.0004 (eq 5 and Table S2). Taking into account this contribution of the deprotonation step to the overall observable N isotope fractionation in DMTA, an apparent kinetic N isotope effect of 1.0025 ± 0.0011 ($AKIE_N^B$; eqs 5 and S2) can be assigned to the reaction of the deprotonated DMTA species. This $AKIE_N^B$ can originate from the nucleophilic substitution reaction of the tertiary amine with NH_2Cl (**2** → **3**), the oxidation of the hydrazine intermediate (**3** → **4**), or a combination there of (**2** ⇌ **3** → **4**). A more rigorous assignment of N isotope fractionation is currently speculative but data for similar reactions such as the N atom oxidation of aromatic *N*-alkylamines, which could mimick reaction **3** → **4**, confirms that N isotope effects following the deprotonation step are indeed small.[57,65] Note that we neglect unknown reactions causing the NDMA yield to be <100%. These side reactions that did not lead to NDMA are more likely caused from reactions of radical intermediates **4** and **5**, which do not affect the N isotope fractionation determined in the reactant.

The results obtained from the chloramination of DMBA were almost identical to those with DMTA despite a smaller molar NDMA yield (58 ± 0.6%, Figure S2 and Table S2). Using a pK_a value of 9.0 for DMBA[66] and the $EIE_N^{BH^+-B}$ obtained for DMTA, the $AKIE_N^B$ associated with the transformation of the deprotonated DMBA (**2**) was 1.0056 ± 0.0007. This value is only slightly larger than the one for DMTA (1.0024 ± 0.0011) and supports the assumption that the chloramination of different tertiary amines proceeds through the same reaction mechanism.

Carbon isotope fractionation in DMTA and DMBA was substantially smaller than that for N (Figures 2b and S2b). The smaller $AKIE_C$s of 1.0021 ± 0.0003 and 1.0014 ± 0.0001 (Table S2) of DMTA and DMBA, respectively, are consistent with the assumptions made for the origins of N isotope fractionation. $EIE_C^{BH^+-B}$ for the deprotonation of $-R_3N^+-H$ bonds are small (≤1.001).[53] Moreover, we found that the methylthiophene-moiety of DMTA did not react with NH_2Cl (Figure S7). Consequently, the reaction with NH_2Cl (**2** → **3**) occurs exclusively at the $N(CH_3)_2$ group of DMTA and DMBA and only involves N atoms. Small changes in $\delta^{13}C$ values of DMTA and DMBA are due to secondary ^{13}C isotope effects of C atoms that are not located at the reactive sites of the tertiary amines.

N Isotope Fractionation in NDMA during the Chloramination of Tertiary Amines. Whereas the C and N isotope fractionation in tertiary amines conveys information on the initial steps of chloramination, the C and N isotope fractionation in NDMA additionally reflects the isotope effects of the subsequent reactions (**4** → → **7**) as well as those to not identified products. We use the data on N isotope fractionation associated with the chloramination of DFUR and DMTA shown in Figures 1b and 2b to speculate about the additional isotope sensitive reactions while neglecting contributions of reactions that do not lead to NDMA. Because DFUR, DMTA, and NH_2Cl all exhibit similar initial $\delta^{15}N$ values (−1‰ to −4‰), the difference of these numbers to the "initial" $\delta^{15}N$ values of NDMA at low NDMA yield (−24‰ to −28‰ at approximately 10% NDMA yield; Table S3) offers qualitative evidence for the cumulative isotope effects of the reactions leading to NDMA. The difference of approximately 20‰ exceeds the theoretical offset of 13‰ that would have been caused from a N isotope effect of 1.0127 (DMTA) for the initial steps of tertiary amine transformation (**1** → → **4**). Reactions **4** → → **7**, therefore, could have caused additional N isotope fractionation but current knowledge is too limited to assign isotope effects to individual steps. Based on the rule of thumb that isotope fractionation increases with the extent of bonding changes,[23] the formation of peroxyl radicals (**4** → **5**) as well as the C−N bond cleavage,[67] and N=O bond formation during the release of NDMA (**6** → **7**) may be primarily responsible for this additional N isotope fractionation in NDMA.

Isotope Fractionation Trends in NDMA as a Proxy for its Formation Pathway. *Effects of the Molecular Structure of Tertiary Amines.* We hypothesize that the ^{13}C and ^{15}N kinetic isotope effects of the many reactions shown in Scheme 1 result in C and N isotope fractionation trends in NDMA that are characteristic for the NDMA formation through chloramination of tertiary amines. Correlations of isotope fractionation are used frequently to identify how a reactant (i.e., an organic contaminant) is transformed (e.g., refs 59 and 68−70). Conversely, the methodology of multielement isotope fractionation is applied only rarely to fingerprint the processes leading to contaminants. Here, we evaluated the linear correlation of C and N isotope fractionation in NDMA from four different precursors, namely ranitidine, DFUR, DMTA, and DMBA.

Figure 3 shows how $\delta^{13}C$ and $\delta^{15}N$ values of NDMA increase during its formation from different precursors and correlations with slopes of $\Delta^{15}N_{NDMA}/\Delta^{13}C_{NDMA}$. The differences of initial $\delta^{13}C$ and $\delta^{15}N$ values of NDMA are due to the different C and N isotope compositions of the precursor compounds (Table S1). The ^{15}N AKIEs are much larger than the ^{13}C AKIEs because only the N atoms of NDMA undergo bond cleavage and bond formation reactions. Consequently, N isotope fractionation in NDMA is substantially larger than C isotope fractionation. The $\Delta^{15}N_{NDMA}/\Delta^{13}C_{NDMA}$ slopes are compiled in Table 1 and

DOI: 10.1021/acs.est.7b03919
Environ. Sci. Technol. 2017, 51, 13170−13179

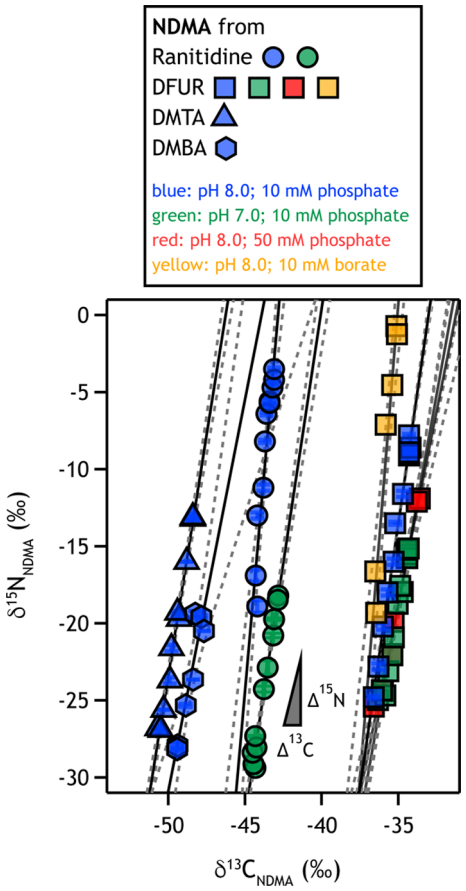

Figure 3. $\delta^{15}N$ vs $\delta^{13}C$ values of NDMA for the chloramination of four different tertiary amines namely ranitidine (3 μM), DFUR (3 μM), DMTA (40 μM), and DMBA (40 μM) in 10 mM phosphate buffer at pH 8.0. Chloramination experiments with ranitidine and DFUR were also conducted in 10 mM phosphate buffer at pH 7.0. NDMA formation from DFUR was further studied in 50 mM phosphate buffer (pH 8.0) and 10 mM borate buffer (pH 8.0). Solid lines represent linear regressions and dashed lines are the corresponding 95% confidence intervals. Standard deviations of triplicate $\delta^{13}C$ and $\delta^{15}N$ measurements of NDMA were <0.4‰ and <0.6‰, respectively, and smaller than marker sizes.

span from 5.1 ± 2.1 to 13 ± 5.0 under identical experimental conditions (that is, pH 8.0 in 10 mM phosphate buffer). Neither the type of precursor molecule nor the molar yield of NDMA (from 58 ± 1% to 97 ± 4%;[29] Table 1 and Figure S5) affects the observed C and N isotope fractionation trend systematically. Except for ranitidine ($\Delta^{15}N_{NDMA}/\Delta^{13}C_{NDMA}$ = 13 ± 0.5), all slopes are identical within uncertainty. Note, however, that these correlations are very sensitive to the extent of C isotope fractionation affecting the $N(CH_3)_2$ and methylene groups. Such secondary C isotope effects of nonreactive moieties are not well understood and we cannot rule out that C isotope fractionation in the $N(CH_3)_2$ moiety of ranitidine differs from that of the other, smaller precursor molecules (Scheme 1).

Impact of Buffer Type and pH. Similar observations regarding the correlation of C and N isotope fractionation in NDMA were made when NDMA was formed from DFUR and ranitidine at pH 7.0 and 8.0 in the presence of different buffers and buffer concentrations (Figure 3, Table 1, and sections S6 and S8). All $\Delta^{15}N_{NDMA}/\Delta^{13}C_{NDMA}$ values derived from experiments in phosphate buffers were confined to a small range (5.0 ± 0.9 to 6.9 ± 0.5) as for NDMA produced from DMTA and DMBA.

Table 1. Molar NDMA Yield (%) as Well as Dual-Isotope Slopes ($\Delta^{15}N_{NDMA}/\Delta^{13}C_{NDMA}$) for the Reaction of DFUR (3 μM), Ranitidine (3 μM), DMTA (40 μM), and DMBA (40 μM) with NH_2Cl (45μM or 600 μM, Respectively) in 10 mM Phosphate Buffer at pH 8.0[a]

	buffer				
precursor	type	mM	pH	molar NDMA yield (%)	$\Delta^{15}N_{NDMA}/\Delta^{13}C_{NDMA}$ (−)[b]
DFUR	phosphate	10	8.0	65 ± 2	6.9 ± 0.5
	phosphate	10	7.0	66 ± 1	5.5 ± 0.6
	phosphate	50	8.0	68 ± 1	5.0 ± 0.9
	borate	10	8.0	88 ± 1	12 ± 3.5
ranitidine	phosphate	10	8.0	97 ± 4	13 ± 5.0
	phosphate	10	7.0	84 ± 0.4	6.6 ± 0.7
DMTA	phosphate	10	8.0	75 ± 0.1	5.1 ± 2.1
DMBA	phosphate	10	8.0	58 ± 1	6.3 ± 0.6

[a]Chloramination experiments with DFUR and ranitidine were conducted using different buffer types and concentrations and pH values. [b]Slope of a linear regression analysis of $\delta^{15}N$ vs $\delta^{13}C$; uncertainties denote 95% confidence intervals.

$\Delta^{15}N_{NDMA}/\Delta^{13}C_{NDMA}$ obtained from experiments in borate buffer, however, were larger and more uncertain (12 ± 3.5).

As shown in Figure S6, we observed an increase of the rates of NDMA formation when increasing the phosphate buffer concentration from 10 to 50 mM at pH 8.0. Conversely, NDMA formation was slower at pH 7.0 (10 mM phosphate buffer; Figures S8 and S9). However, none of these variations of reaction rates affected the $\Delta^{15}N_{NDMA}/\Delta^{13}C_{NDMA}$ value systematically. This finding is consistent with previous studies that showed that water matrix components, presumably natural organic matter, can slow down the formation of NDMA during chloramination of ranitidine without affecting the molar NDMA yield.[71] Even though we cannot explain some of the variations, our data suggests that the combined C and N isotope fractionation trends in NDMA can serve as an indicator for the NDMA formation pathway during chloramination.

IMPLICATIONS FOR STABLE ISOTOPE ANALYSIS OF NDMA DURING WATER DISINFECTION

Our study provides the first evidence that isotope fractionation trends from several elements in NDMA may reflect its formation pathway. Even though the isotope effects of some of the reactions leading to NDMA are not yet known, the chloramination of a series of tertiary amines under slightly different reaction conditions resulted in a consistent pattern of C and N isotope fractionation in NDMA. Further work is warranted to confine correlations of C and N isotope fractionation in NDMA for chloramination reactions shown here, for example, by taking into account effects of water constituents and water quality. While our work focused on the comparison of isotope fractionation of elements at reactive versus nonreactive positions, that is, primary N versus secondary C isotope effects, additional information on the mechanisms of NDMA formation may be obtained from oxygen isotopes in NDMA. The oxygenation of N atoms of the precursor compounds is a critical step in the NDMA formation pathway[35] and oxygen isotope fractionation may be larger than what we showed here for C and H isotopes. Given that NDMA formation mechanisms have been shown to vary depending on the precursor and disinfectant,[17] systematic investigations of the isotope fractionation behavior of NDMA formed through different pathways, with other disinfectants,

DOI: 10.1021/acs.est.7b03919
Environ. Sci. Technol. 2017, 51, 13170−13179

and over the entire range of observed NDMA yields and concentration ranges may lead to a new tool for the identification of NDMA formation during water treatment processes.

■ ASSOCIATED CONTENT

Supporting Information

The Supporting Information is available free of charge on the ACS Publications website at DOI: 10.1021/acs.est.7b03919.

Additional details on safety considerations, a list of all chemicals, reference isotope signatures, and a list and detailed description of the determination of isotope enrichment factors and kinetic isotope effects. Figures illustrating method quantification limits, isotope fractionation, the determination of bulk isotope enrichment factors and ^{15}N equilibrium isotope effects, reaction kinetics, the impact of buffer type and concentration as well as pH, and the chloramination of 2-thiophenemethanol. (PDF)

■ AUTHOR INFORMATION

Corresponding Author

*E-mail: thomas.hofstetter@eawag.ch.

ORCID

Thomas B. Hofstetter: 0000-0003-1906-367X

Present Address

‖S.S.: Civil and Environmental Engineering, Stanford University, Stanford, CA 94305, USA.

Notes

The authors declare no competing financial interest.

■ ACKNOWLEDGMENTS

This work was supported by the Swiss National Science Foundation (project no. 200021-140545). We thank Jakov Bolotin for analytical support, Christine Egli for help with laboratory experiments, and Sarah Pati and Olaf A. Cirpka for valuable discussions.

■ REFERENCES

(1) Richardson, S. D.; Plewa, M. J.; Wagner, E. D.; Schoeny, R.; DeMarini, D. M. Occurrence, genotoxicity, and carcinogenicity of regulated and emerging disinfection by-products in drinking water: A review and roadmap for research. *Mutat. Res., Rev. Mutat. Res.* **2007**, *636*, 178−242.

(2) United States Environmental Protection Agency Office of Research and Development; National Center for Environmental Assessment; Integrated Risk Information System Technical Fact Sheet: *N*-Nitrosodimethylamine. www.epa.gov/fedfac/technical-fact-sheet-n-nitroso-dimethylamine-ndma (accessed June 28, 2016).

(3) Russell, C. G.; Blute, N. K.; Via, S.; Wu, X.; Chowdhury, Z. Nationwide assessment of nitrosamine occurrence and trends. *J. Am. Water Works Ass.* **2012**, *104*, 205−217.

(4) Charrois, J. W. A.; Boyd, J. M.; Froese, K. L.; Hrudey, S. E. Occurrence of *N*-nitrosamines in Alberta public drinking-water distribution systems. *J. Environ. Eng. Sci.* **2007**, *6*, 103−114.

(5) Woods, G. C.; Dickenson, E. R. V. Evaluation of final UCMR2 database: Nationwide trend in NDMA. *J. Am. Water Works Ass.* **2015**, *107*, E58−E68.

(6) Wert, E. C.; Rosario-Ortiz, F. L. Intracellular organic matter from cyanobacteria as a precursor for carbonaceous and nitrogenous disinfection byproducts. *Environ. Sci. Technol.* **2013**, *47*, 6332−6340.

(7) Kristiana, I.; Tan, J.; Joll, C. A.; Heitz, A.; von Gunten, U.; Charrois, J. W. Formation of *N*-nitrosamines from chlorination and chloramination of molecular weight fractions of natural organic matter. *Water Res.* **2013**, *47*, 535−546.

(8) Chen, Z.; Valentine, R. L. Formation of *N*-nitrosodimethylamine (NDMA) from humic substances in natural water. *Environ. Sci. Technol.* **2007**, *41*, 6059−6065.

(9) Dotson, A.; Westerhoff, P.; Krasner, S. Nitrogen enriched dissolved organic matter (DOM) isolates and their affinity to form emerging disinfection by-products. *Water Sci. Technol.* **2009**, *60*, 135−143.

(10) Schmidt, C. K.; Brauch, H.-J. *N,N*-Dimethylsulfamide as precursor for *N*-nitrosodimethylamine (NDMA) formation upon ozonation and its fate during drinking water treatment. *Environ. Sci. Technol.* **2008**, *42*, 6340−6346.

(11) Le Roux, J.; Gallard, H.; Croue, J.-P. Chloramination of nitrogenous contaminants (pharmaceuticals and pesticides): NDMA and halogenated DBPs formation. *Water Res.* **2011**, *45*, 3164−3174.

(12) von Gunten, U.; Salhi, E.; Schmidt, C. K.; Arnold, W. A. Kinetics and mechanisms of *N*-nitrosodimethylamine formation upon ozonation of *N,N*-dimethylsulfamide-containing waters: Bromide catalysis. *Environ. Sci. Technol.* **2010**, *44*, 5762−5768.

(13) Oya, M.; Kosaka, K.; Asami, M.; Kunikane, S. Formation of *N*-nitrosodimethylamine (NDMA) by ozonation of dyes and related compounds. *Chemosphere* **2008**, *73*, 1724−1730.

(14) Shen, R.; Andrews, S. A. Demonstration of 20 pharmaceuticals and personal care products (PPCPs) as nitrosamine precursors during chloramine disinfection. *Water Res.* **2011**, *45*, 944−952.

(15) Park, S.-H.; Wei, S.; Mizaikoff, B.; Taylor, A. E.; Favero, C.; Huang, C.-H. Degradation of amine-based water treatment polymers during chloramination as *N*-nitrosodimethylamine (NDMA) precursors. *Environ. Sci. Technol.* **2009**, *43*, 1360−1366.

(16) Padhye, L.; Luzinova, Y.; Cho, M.; Mizaikoff, B.; Kim, J. H.; Huang, C. H. PolyDADMAC and dimethylamine as precursors of N-nitrosodimethylamine during ozonation: Reaction kinetics and mechanisms. *Environ. Sci. Technol.* **2011**, *45*, 4353−4359.

(17) Shah, A. D.; Mitch, W. A. Halonitroalkanes, halonitriles, haloamides, and *N*-nitrosamines: A critical review of nitrogenous disinfection byproduct formation pathways. *Environ. Sci. Technol.* **2012**, *46*, 119−131.

(18) Bond, T.; Templeton, M. R.; Graham, N. Precursors of nitrogenous disinfection by-products in drinking water - A critical review and analysis. *J. Hazard. Mater.* **2012**, *235*−*236*, 1−16.

(19) Arnold, W. A.; Bolotin, J.; von Gunten, U.; Hofstetter, T. B. Evaluation of functional groups responsible for chloroform formation during water chlorination using compound specific isotope analysis. *Environ. Sci. Technol.* **2008**, *42*, 7778−7785.

(20) Breider, F.; Hunkeler, D. Mechanistic insights into the formation of chloroform from natural organic matter using stable carbon isotope analysis. *Geochim. Cosmochim. Acta* **2014**, *125*, 85−95.

(21) Breider, F.; Albers, C. N.; Hunkeler, D. Assessing the role of trichloroacetyl-containing compounds in the natural formation of chloroform using stable carbon isotopes analysis. *Chemosphere* **2013**, *90*, 441−448.

(22) Kohen, A.; Limbach, H.-H. *Isotope Effects in Chemistry and Biology*; Taylor & Francis: New York, 2006.

(23) Wolfsberg, M.; Hook, W. A. V.; Paneth, P.; Rebelo, L. P. N. *Isotope Effects in Chemical, Geological, and Bio Sciences*; Springer: Heidelberg, Germany, 2010.

(24) Elsner, M.; Jochmann, M. A.; Hofstetter, T. B.; Hunkeler, D.; Bernstein, A.; Schmidt, T. C.; Schimmelmann, A. Current challenges in compound-specific stable isotope analysis of environmental organic contaminants. *Anal. Bioanal. Chem.* **2012**, *403*, 2471−2491.

(25) Elsner, M. Stable isotope fractionation to investigate natural transformation mechanisms of organic contaminants: Principles, prospects and limitations. *J. Environ. Monit.* **2010**, *12*, 2005−2031.

(26) Hofstetter, T. B.; Schwarzenbach, R. P.; Bernasconi, S. M. Assessing transformation processes of organic compounds using stable isotope fractionation. *Environ. Sci. Technol.* **2008**, *42*, 7737−7743.

(27) Hofstetter, T. B.; Berg, M. Assessing transformation processes of organic contaminants by compound-specific stable isotope analyses. *TrAC, Trends Anal. Chem.* **2011**, *30*, 618−627.

(28) Aelion, C. M.; Höhener, P.; Hunkeler, D.; Aravena, R. *Environnmental Isotopes in Biodegradationand Bioremediation*; Taylor & Francis Group: Boca Raton, FL, 2010.
(29) Spahr, S.; Bolotin, J.; Schleucher, J.; Ehlers, I.; von Gunten, U.; Hofstetter, T. B. Compound-specific carbon, nitrogen, and hydrogen isotope analysis of *N*-nitrosodimethylamine in aqueous solutions. *Anal. Chem.* **2015**, *87*, 2916−2924.
(30) Pati, S. G.; Kohler, H.-P. E.; Pabis, A.; Paneth, P.; Parales, R. E.; Hofstetter, T. B. Substrate and enzyme specificity of the kinetic isotope effects associated with the dioxygenation of nitroaromatic contaminantsnzyme. *Environ. Sci. Technol.* **2016**, *50*, 6708−6716.
(31) Pati, S. G.; Kohler, H.-P. E.; Bolotin, J.; Parales, R. E.; Hofstetter, T. B. Isotope effects of enzymatic dioxygenation of nitrobenzene and 2-nitrotoluene by nitrobenzene dioxygenase. *Environ. Sci. Technol.* **2014**, *48*, 10750−10759.
(32) Elsner, M.; Chartrand, M.; VanStone, N.; Couloume, G. L.; Sherwood Lollar, B. Identifying abiotic chlorinated ethene degradation: Characteristic isotope patterns in reaction products with nanoscale zero-valent iron. *Environ. Sci. Technol.* **2008**, *42*, 5963−5970.
(33) Mariotti, A.; Germon, J. C.; Hubert, P.; Kaiser, P.; Letolle, R.; Tardieux, A.; Tardieux, P. Experimental determination of nitrogen kinetic isotope fractionation - Some principles - Illustration for the denitrification and ntrification processes. *Plant Soil* **1981**, *62*, 413−430.
(34) Hartenbach, A.; Hofstetter, T. B.; Berg, M.; Bolotin, J.; Schwarzenbach, R. P. Using nitrogen isotope fractionation to assess abiotic reduction of nitroaromatic compounds. *Environ. Sci. Technol.* **2006**, *40*, 7710−7716.
(35) Spahr, S.; Cirpka, O. A.; von Gunten, U.; Hofstetter, T. B. Formation of *N*-nitrosodimethylamine during chloramination of secondary and tertiary amines: Role of molecular oxygen and radical intermediates. *Environ. Sci. Technol.* **2017**, *51*, 280−290.
(36) Hayes, J. M. In *Stable Isotopic Geochemistry*; Valley, J., Cole, D. R., Eds.; Mineralogical Society of America: Chantilly, VA, 2001; Vol. *43*.
(37) Dauphas, N.; Schauble, E. A. Mass fractionation laws, mass-independent effects, and isotopic anomalies. *Annu. Rev. Earth Planet. Sci.* **2016**, *44*, 709−783.
(38) Luz, B.; Barkan, E. Assessment of oceanic productivity with the triple-isotope composition of dissolved oxygen. *Science* **2000**, *288*, 2028−2031.
(39) Tostevin, R.; Turchyn, A. V.; Farquhar, J.; Johnston, D. T.; Eldridge, D. L.; Bishop, J. K. B.; McIlvin, M. R. Multiple sulfur isotope constraints on the modern sulfur cycle. *Earth Planet. Sci. Lett.* **2014**, *396*, 14−21.
(40) Bao, H. Sulfate: A time capsule for Earth's O_2, O_3, and H_2O. *Chem. Geol.* **2015**, *395*, 108−118.
(41) Bao, H.; Cao, X.; Hayles, J. A. Triple oxygen isotopes: Fundamental relationships and applications. *Annu. Rev. Earth Planet. Sci.* **2016**, *44*, 463−492.
(42) Johnston, D. T. Multiple sulfur isotopes and the evolution of Earth's surface sulfur cycle. *Earth-Sci. Rev.* **2011**, *106*, 161−183.
(43) Franz, H. B.; Kim, S. T.; Farquhar, J.; Day, J. M. D.; Economos, R. C.; McKeegan, K. D.; Schmitt, A. K.; Irving, A. J.; Hoek, J.; Dottin, J., III Isotopic links between atmospheric chemistry and the deep sulphur cycle on Mars. *Nature* **2014**, *508*, 364−368.
(44) Le Roux, J.; Gallard, H.; Croue, J.-P.; Papot, S.; Deborde, M. NDMA formation by chloramination of ranitidine: Kinetics and mechanisms. *Environ. Sci. Technol.* **2012**, *46*, 11095−11103.
(45) Liu, Y. D.; Selbes, M.; Zeng, C.; Zhong, R.; Karanfil, T. Formation mechanism of NDMA from ranitidine, trimethylamine, and other tertiary amines during chloramination: A computational study. *Environ. Sci. Technol.* **2014**, *48*, 8653−8663.
(46) Schreiber, I. M.; Mitch, W. A. Nitrosamine formation pathway revisited: The importance of chloramine speciation and dissolved oxygen. *Environ. Sci. Technol.* **2006**, *40*, 6007−6014.
(47) Selbes, M.; Kim, D.; Ates, N.; Karanfil, T. The roles of tertiary amine structure, background organic matter and chloramine species on NDMA formation. *Water Res.* **2013**, *47*, 945−953.
(48) Valentine, R. L.; Brandt, K. I.; Jafvert, C. T. A spectrophotometric study of the formation of an unidentified monochloramine decomposition product. *Water Res.* **1986**, *20*, 1067−1074.
(49) Soltermann, F.; Lee, M.; Canonica, S.; von Gunten, U. Enhanced *N*-nitrosamine formation in pool water by UV irradiation of chlorinated secondary amines in the presence of monochloramine. *Water Res.* **2013**, *47*, 79−90.
(50) Böhlke, J. K.; Gwinn, C. J.; Coplen, T. B. New reference materials for nitrogen-isotope-ratio measurements. *Geostand. Geoanal. Res.* **1993**, *17*, 159−164.
(51) Soulard, M.; Bloc, F.; Hatterer, A. Diagrams of existence of chloramines and bromamines in aqueous solution. *J. Chem. Soc., Dalton Trans.* **1981**, 2300−2310.
(52) Pinkernell, U.; Nowack, B.; Gallard, H.; von Gunten, U. Methods for the photometric determination of reactive bromine and chlorine species with ABTS. *Water Res.* **2000**, *34*, 4343−4350.
(53) Skarpeli-Liati, M.; Arnold, W. A.; Turgeon, A.; Cramer, C. J.; Hofstetter, T. B.; Garr, A. N. pH-Dependent equilibrium isotope fractionation associated with compound-specific nitrogen and carbon isotope analysis by SPME-GC/IRMS. *Anal. Chem.* **2011**, *83*, 1641−1648.
(54) Jochmann, M. A.; Blessing, M.; Haderlein, S. B.; Schmidt, T. C. A new approach to determine method detection limits for compound-specific isotope analysis of volatile organic compounds. *Rapid Commun. Mass Spectrom.* **2006**, *20*, 3639−3648.
(55) Schimmelmann, A.; Albertino, A.; Sauer, P. E.; Qi, H.; Molinie, R.; Mesnard, F. Nicotine, acetanilide and urea multi-level ^{2}H-, ^{13}C- and ^{15}N-abundance reference materials for continuous-flow isotope ratio mass spectrometry. *Rapid Commun. Mass Spectrom.* **2009**, *23*, 3513−3521.
(56) Schimmelmann, A.; Lewan, M. D.; Wintsch, R. P. D/H isotope ratios of kerogen, bitumen, oil, and water in hydrous pyrolysis of source rocks containing kerogen types I, II, IIS, and III. *Geochim. Cosmochim. Acta* **1999**, *63*, 3751−3766.
(57) Skarpeli-Liati, M.; Jiskra, M.; Turgeon, A.; Garr, A. N.; Arnold, W. A.; Cramer, C. J.; Schwarzenbach, R. P.; Hofstetter, T. B. Using nitrogen isotope fractionation to assess the oxidation of substituted anilines by manganese oxide. *Environ. Sci. Technol.* **2011**, *45*, 5596−5604.
(58) Le Roux, J.; Gallard, H.; Croue, J.-P. Formation of NDMA and halogenated DBPs by chloramination of tertiary amines: The influence of bromide ion. *Environ. Sci. Technol.* **2012**, *46*, 1581−1589.
(59) Pati, S. G.; Shin, K.; Skarpeli-Liati, M.; Bolotin, J.; Eustis, S. N.; Spain, J. C.; Hofstetter, T. B. Carbon and nitrogen isotope effects associated with the dioxygenation of aniline and diphenylamine. *Environ. Sci. Technol.* **2012**, *46*, 11844−11853.
(60) Wijker, R. S.; Adamczyk, P.; Bolotin, J.; Paneth, P.; Hofstetter, T. B. Isotopic analysis of oxidative pollutant degradation pathways exhibiting large H isotope fractionation. *Environ. Sci. Technol.* **2013**, *47*, 13459−13468.
(61) Elsner, M.; McKelvie, J.; Lacrampe-Couloume, G.; Sherwood Lollar, B. Insight into methyl tert-butyl ether (MTBE) stable isotope fractionation from abiotic reference experiments. *Environ. Sci. Technol.* **2007**, *41*, 5693−5700.
(62) Choi, J.; Valentine, R. L. Formation of *N*-nitrosodimethylamine (NDMA) from reaction of monochloramine: A new disinfection by-product. *Water Res.* **2002**, *36*, 817−824.
(63) Rishavy, M. A.; Cleland, W. W. ^{13}C, ^{15}N, and ^{18}O equilibrium isotope effects and fractionation factors. *Can. J. Chem.* **1999**, *77*, 967−977.
(64) Tanaka, N.; Hosoya, K.; Nomura, K.; Yoshimura, T.; Ohki, T.; Yamaoka, R.; Kimata, K.; Araki, M. Separation of nitrogen and oxygen isotopes by liquid chromatography. *Nature* **1989**, *341*, 727−728.
(65) Skarpeli-Liati, M.; Pati, S. G.; Bolotin, J.; Eustis, S. N.; Hofstetter, T. B. Carbon, hydrogen, and nitrogen isotope fractionation associated with oxidative transformation of substituted aromatic N-alkyl amines. *Environ. Sci. Technol.* **2012**, *46*, 7189−7198.
(66) Rosenblatt, D. H.; Hull, L. A.; De Luca, D. C.; Davis, G. T.; Weglein, R. C.; Williams, H. K. R. Oxidations of amines. II. Substituent effects in chlorine dioxide oxidations. *J. Am. Chem. Soc.* **1967**, *89*, 1158−1163.

DOI: 10.1021/acs.est.7b03919
Environ. Sci. Technol. 2017, 51, 13170−13179

(67) Marlier, J. F.; Cleland, W. W. Multiple isotope effect study of the hydrolysis of formamide by urease from Jack Bean (*Canavalia ensiformis*). *Biochemistry* **2006**, *45*, 9940−9948.
(68) Wijker, R. S.; Bolotin, J.; Nishino, S. F.; Spain, J. C.; Hofstetter, T. B. Using compound-specific isotope analysis to assess biodegradation of nitroaromatic explosives in the subsurface. *Environ. Sci. Technol.* **2013**, *47*, 6872−6883.
(69) Reinnicke, S.; Simonsen, A.; Sörensen, S. R.; Aamand, J.; Elsner, M. C and N isotope fractionation during biodegradation of the pesticide metabolite 2,6-dichlorobenzamide (BAM): Potential for environmental assessments. *Environ. Sci. Technol.* **2012**, *46*, 1447−1454.
(70) Wijker, R. S.; Zeyer, J.; Hofstetter, T. B. Isotope fractionation associated with the simultaneous biodegradation of multiple nitrophenol isomers by *Pseudomonas putida* B2. *Environ. Sci.: Process Impacts* **2017**, *19*, 775−784.
(71) Shen, R.; Andrews, S. A. NDMA formation kinetics from three pharmaceuticals in four water matrices. *Water Res.* **2011**, *45*, 5687−5694.

DOI: 10.1021/acs.est.7b03919
Environ. Sci. Technol. 2017, 51, 13170−13179